Contents lists available at ScienceDirect

Systems & Control Letters

journal homepage: www.elsevier.com/locate/sysconle

systems &
control letters
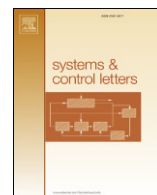
Controlling Neimark–Sacker bifurcations in discrete-time multivariable systems ☆

María Belén D'Amico [a,b,∗], Guanrong Chen [c], Eduardo E. Paolini [a], Jorge L. Moiola [a,b]

[a] Instituto de Investigaciones en Ingeniería Eléctrica "Alfredo Desages", Dto. de Ingeniera Eléctrica y de Computadoras, Universidad Nacional del Sur, Avda Alem 1253, B8000CPB Bahía Blanca, Argentina
[b] Consejo Nacional de Investigaciones Científicas y Técnicas, Argentina
[c] Department of Electronic Engineering, City University of Hong Kong, Kowloon, Hong Kong, China

ARTICLE INFO

ABSTRACT

A novel method is presented for controlling the amplitudes and stability of orbits generated from Neimark–Sacker bifurcations in discrete-time systems. The technique is rooted in the frequency-domain approach for the study of bifurcations in maps.

© 2009 Elsevier B.V. All rights reserved.

1. Introduction

Oscillations appear frequently in many dynamical systems. For that reason, scientists have been developing methods and algorithms for analyzing and even controlling them. It has been demonstrated that one of the most common causes of this phenomenon is the existence of certain bifurcations [1]. In continuous-time systems, oscillations appear mainly due to Hopf bifurcations. In discrete-time systems, however, the essential cause is Neimark–Sacker (N–S) bifurcation or period-doubling bifurcation.

Since bifurcations are related to the presence of nonlinearities in the system, linear control methods are inadequate for changing their characteristics. A proper way of obtaining some desirable dynamical behaviors is to use *bifurcation control techniques* [2–4]. Typical control objectives concerning oscillations are to relocate the birth of a bifurcation to other parameter values, to enlarge/reduce their amplitudes or to modify their stability. When applying bifurcation control, it is usually required to preserve the location and/or stability of the fixed points, so as to continue the

original operation modes. This requirement can be met by using homogeneous polynomials [5,6], highpass ("washout") filters [7,8], and some other techniques.

Bifurcation control research has evolved progressively and systematically since the pioneering work of [9,10]. In particular, several effective methods have been developed for discrete-time systems. For example, stabilization of period-doubling bifurcations is examined in [11], where both static and dynamic controllers are discussed. A technique to deal with N–S bifurcations is presented in [12]. These results complement those given in [13], in which stabilization is accomplished by using quadratic functions. Other methods related to the control or even anti-control of bifurcations in maps can be found in [5,14–18].

Most of these results are derived by applying the center manifold theorem and the normal form theory, using a state-space representation of the system. An alternative method for analyzing N–S bifurcations from a frequency-domain (FD) viewpoint is proposed in [19,20]. Unlike the classical absolute stability criteria for input–output systems presented in [21–23], this method not only determines the critical condition for the existence of the bifurcation but also provides approximations of the emerging orbits via the Nyquist stability criterion, the harmonic balance method and Fourier series analysis.

The aim of this paper is to show the potential of the FD approach in the design of nonlinear control laws which modify the characteristics of the oscillations but preserve the location and stability of the fixed points. Two alternatives are shown: a dynamic controller using washout filters to dissociate the control from the equilibria, and a static controller using ad-hoc nonlinear functions.
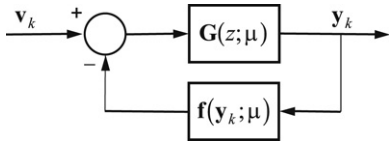
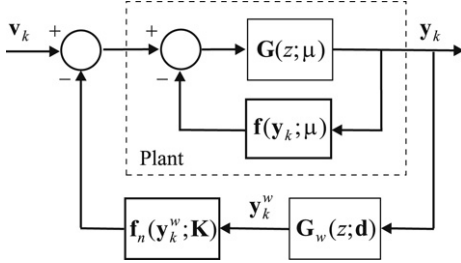**Fig. 1.** Nonlinear discrete-time input–output system.

Fig. 2. Block diagram of the dynamic feedback controller.

A first attempt to control a N–S bifurcation using the FD method has been reported in [24] but the present article enhances the scope and applications.

The paper is organized as follows. In Section 2, the FD approach for the analysis of N–S bifurcations is reviewed. In Section 3, two methods for controlling N–S bifurcations are presented. An example is developed in Section 4. Some concluding remarks are given in Section 5.

2. Preliminaries

Consider the input–output discrete-time multivariable system S shown in Fig. 1 consisting of a closed-loop connection between a linear block defined by an $m \times \ell$ rational transfer matrix $\mathbf{G}(\cdot)$, and a memoryless nonlinear block given by a smooth (C^r with $r \geq 3$) function $\mathbf{f} : \mathbf{R}^m \times \mathbf{R}^s \to \mathbf{R}^\ell$. In the figure, $\boldsymbol{\mu} \in \mathbf{R}^s$ is the parameter vector, z is the complex variable of the z-transform, $\mathbf{v}_k \in \mathbf{R}^\ell$ is the input (assumed to be $\mathbf{0}$) and $\mathbf{y}_k \in \mathbf{R}^m$ is the output.

Theorem 1. *Let $\widehat{\mathbf{y}}$ be a fixed point of S given by $\widehat{\mathbf{y}} = -\mathbf{G}(1; \boldsymbol{\mu})\mathbf{f}(\widehat{\mathbf{y}}; \boldsymbol{\mu})$. The dynamical behavior of S in a neighborhood of $\widehat{\mathbf{y}}$ is characterized as follows. Let $\widehat{\lambda}(e^{i\omega}; \boldsymbol{\mu})$ be one eigenvalue of $\mathbf{G}(z; \boldsymbol{\mu})\mathbf{J}(\boldsymbol{\mu})$ with $\mathbf{J}(\boldsymbol{\mu}) = D_{\mathbf{y}}\mathbf{f}(\widehat{\mathbf{y}}; \boldsymbol{\mu})$[1] for $z = e^{i\omega}$ whose Nyquist diagram crosses the critical point $-1 + i0$ at $\boldsymbol{\mu} = \boldsymbol{\mu}_o$ and $\omega = \omega_o$, with $e^{in\omega_o} \neq 1$ for $n = 1, 2, 3, 4$. If $-1 + \xi(\omega; \boldsymbol{\mu})\theta^2$, with $\xi(\omega; \boldsymbol{\mu}) \neq 0$ (see Table 1) intersects $\widehat{\lambda}(e^{i\omega}; \boldsymbol{\mu})$ at a single point for $\boldsymbol{\mu}_R \neq \boldsymbol{\mu}_o$, then system S presents a emerging orbit around $\widehat{\mathbf{y}}$ for $\boldsymbol{\mu}_R$. The stability of the resulting N–S bifurcation is given by index σ (see Table 1).*

Proof. See References [19,20]. The proof is based on the technique first proposed in [25], and extended in [26] for the analysis of Hopf bifurcations in multivariable continuous-time systems. □

The FD technique is not restricted to systems of the form of Fig. 1. A map $\mathbf{x}_{k+1} = \mathbf{A}\mathbf{x}_k + \mathbf{B}\mathbf{g}(\mathbf{x}_k; \boldsymbol{\mu})$ with $\mathbf{x}_k \in \mathbf{R}^n$, $\mathbf{A} \in \mathbf{R}^{n \times n}$ (which may be $\mathbf{0}$), $\mathbf{B} \in \mathbf{R}^{n \times \ell}$ and $\mathbf{g} : \mathbf{R}^m \times \mathbf{R}^s \to \mathbf{R}^\ell$ can always be transformed in a system S by choosing $\mathbf{G}(z; \boldsymbol{\mu}) = \mathbf{C}[z\mathbf{I} - (\mathbf{A} + \mathbf{BDC})]^{-1}\mathbf{B}$ and $\mathbf{f}(\mathbf{y}_k; \boldsymbol{\mu}) = \mathbf{D}\mathbf{y}_k - \mathbf{g}(\mathbf{y}_k; \boldsymbol{\mu})$ where $\mathbf{y}_k = \mathbf{C}\mathbf{x}_k$ and $\mathbf{C} \in \mathbf{R}^{m \times n}$, $\mathbf{D} \in \mathbf{R}^{\ell \times m}$ are arbitrary. The representation is not unique and with the proper selection of $\mathbf{C}$ and $\mathbf{D}$, the dimensions m of the input space and ℓ of the output space of the equivalent system can

---

[1] For the sake of simplicity, $D_{\mathbf{y}}\mathbf{f}(\widehat{\mathbf{y}}; \boldsymbol{\mu})_{ij} = \{\partial f_i(\mathbf{y}; \boldsymbol{\mu})/\partial y_j\}\big|_{\mathbf{y}=\widehat{\mathbf{y}}}$ with $\mathbf{f}(\cdot) = [f_1(\cdot) \ldots f_\ell(\cdot)]^T$ and $\mathbf{y} = [y_1 \ldots y_m]^T$; similar expressions will be used for higher-order derivatives.

Table 1
Frequency-domain analysis of the orbits emerging from a N–S bifurcation.

Step 0	$\mathbf{G}(\cdot), \mathbf{f}(\cdot), \widehat{\mathbf{y}}, \mathbf{J}(\cdot)$ and $\widehat{\lambda}(\cdot)$ such that $\widehat{\lambda}(e^{i\omega_o}; \boldsymbol{\mu}_o) = -1 + i0$ are known.
Step 1	Calculate the left and right eigenvectors associated with $\widehat{\lambda}(e^{i\omega}; \boldsymbol{\mu})$, $\mathbf{u}^T\mathbf{G}(e^{i\omega}; \boldsymbol{\mu})\mathbf{J}(\boldsymbol{\mu}) = \mathbf{u}^T\widehat{\lambda}(e^{i\omega}; \boldsymbol{\mu}), \qquad \mathbf{G}(e^{i\omega}; \boldsymbol{\mu})\mathbf{J}(\boldsymbol{\mu})\mathbf{v} = \widehat{\lambda}(e^{i\omega}; \boldsymbol{\mu})\mathbf{v}.$
Step 2	Evaluate matrix $\mathbf{H}(z; \boldsymbol{\mu}) = [\mathbf{I} + \mathbf{G}(z; \boldsymbol{\mu})\mathbf{J}(\boldsymbol{\mu})]^{-1}\mathbf{G}(z; \boldsymbol{\mu}).$
Step 3	Build matrices $\mathbf{Q} = D_{\mathbf{y}}^2\mathbf{f}(\widehat{\mathbf{y}}; \boldsymbol{\mu})\mathbf{v}$ and $\mathbf{L} = D_{\mathbf{y}}^3\mathbf{f}(\widehat{\mathbf{y}}; \boldsymbol{\mu})\mathbf{v} \otimes \mathbf{v}$ as $q_{ij} = \sum_{p=1}^m D_{y_p y_j}^2 f_i(\widehat{\mathbf{y}}; \boldsymbol{\mu})v^p, \qquad l_{ij} = \sum_{p=1}^m \sum_{q=1}^m D_{y_p y_q y_j}^3 f_i(\widehat{\mathbf{y}}; \boldsymbol{\mu})v^p v^q,$ where $i = 1, \ldots, \ell, j = 1, \ldots, m$, and v^p, v^q, $f_i(\cdot)$ are the components of $\mathbf{v}$ and $\mathbf{f}(\cdot)$, respectively. Symbol "$\otimes$" is the tensor product operator.
Step 4	Find vectors $\mathbf{v}_0 = -\mathbf{H}(1; \boldsymbol{\mu})\mathbf{Q}\overline{\mathbf{v}}/4$, $\mathbf{v}_2 = -\mathbf{H}(e^{i2\omega}; \boldsymbol{\mu})\mathbf{Q}\mathbf{v}/4$ and $\mathbf{p}(\omega; \boldsymbol{\mu}) = \mathbf{Q}\mathbf{v}_0 + \overline{\mathbf{Q}}\mathbf{v}_2/2 + \mathbf{L}\overline{\mathbf{v}}/8.$ Symbol "$\overline{\cdot}$" is the complex conjugate operator.
Step 5	Obtain $\xi(\omega; \boldsymbol{\mu}) = -\mathbf{u}^T\mathbf{G}(e^{i\omega}; \boldsymbol{\mu})\mathbf{p}(\omega; \boldsymbol{\mu})/(\mathbf{u}^T\mathbf{v}).$
Step 6	Find ω_R and θ_R from $\widehat{\lambda}(e^{i\omega}; \boldsymbol{\mu}) = -1 + \xi(\omega; \boldsymbol{\mu})\theta^2$ for $\boldsymbol{\mu}_R \neq \boldsymbol{\mu}_o$. If the solution exists, go to Step 7; otherwise, end the procedure.
Step 7	Evaluate $\mathbf{Y}_0 = \theta_R^2\mathbf{v}_0$, $\mathbf{Y}_1 = \theta_R\mathbf{v}$ and $\mathbf{Y}_2 = \theta_R^2\mathbf{v}_2$, and approximate the orbit as $\mathbf{y}_k = \widehat{\mathbf{y}} + \text{Re}\{\mathbf{Y}_0 + \mathbf{Y}_1 e^{i\omega_R k} + \mathbf{Y}_2 e^{i2\omega_R k}\}.$
Step 8	Calculate $\sigma = \text{Re}\{\boldsymbol{\gamma}\,\mathbf{p}(\omega; \boldsymbol{\mu})\}$, $\boldsymbol{\gamma} = \mathbf{u}^T\mathbf{G}(e^{i\omega}; \boldsymbol{\mu})/[e^{i\omega}\mathbf{u}^T D_z \mathbf{G}(e^{i\omega}; \boldsymbol{\mu})\mathbf{J}(\boldsymbol{\mu})\mathbf{v}]$ at $\boldsymbol{\mu} = \boldsymbol{\mu}_o$ and $\omega = \omega_o$. If $\sigma > 0$ ($\sigma < 0$), the orbit is stable (unstable) and the bifurcation is said to be supercritical (subcritical). If σ vanishes, the bifurcation degenerates and the global behavior will be more complex [20].

generally be made smaller than n. If such reduction is achieved, bifurcation analysis in the frequency-domain could be easier to perform than that in time-domain (in spite of the cumbersome expressions of Table 1). The implications of controllability and/or observability in the transformation and analysis of the map in the FD can be found in [26,27].

3. Bifurcation control in the frequency-domain

Suppose system S experiments a N–S bifurcation. The emerging orbits, while preserving the location and stability of the fixed points, can be modified by using a *nonlinear dynamic feedback controller* or even a *nonlinear static feedback controller*. In the first case, the implementation of some highpass filters dissociates the control action from the equilibria. In the second case, the design of the control law is more demanding because it requires exact knowledge of all the equilibrium points to preserve their characteristics.

3.1. Dynamic controller

An outer loop is connected to the original system as shown in Fig. 2. The following results are a formalization of those previously reported in [24].

Assumption DC1. The dynamic block $\mathbf{G}_w(z; \mathbf{d})$ of Fig. 2 is a $m \times m$ diagonal matrix where the nonzero elements are scalar stable highpass filters of the form $g_{ii}(z; d_i) = (z - 1)/(z - 1 + d_i)$ with $i = 1, \ldots, m$, and $d_i \in (0, 2)$.

In general, d_i is chosen such that the cut-off frequency of the highpass filter is smaller than the frequency of oscillation of S.

Assumption DC2. The static function $\mathbf{f}_n(\mathbf{y}_k^w; \mathbf{K}) : \mathbf{R}^m \times \mathbf{R}^v \to \mathbf{R}^\ell$ of Fig. 2 satisfies: (i) it is at least C^3 in its first argument; (ii) $\mathbf{f}_n(\mathbf{0}; \mathbf{K}) = \mathbf{0}$; (iii) $D_y\mathbf{f}_n(\mathbf{0}; \mathbf{K}) = \mathbf{0}$.

For instance, if $\mathbf{y}_k^w = [y_k^{w,1} \quad y_k^{w,2}]^T$, $\mathbf{f}_n(\cdot)$ could be a homogeneous polynomial (with the linear and independent coefficients equal to zero) of the form $\mathbf{f}_n(\mathbf{y}_k^w; \mathbf{K}) = \kappa_1(y_k^{w,1})^2 + \kappa_2(y_k^{w,2})^2 + \kappa_3 y_k^{w,1} y_k^{w,2}$ with $\mathbf{K}$ as the gain vector $\mathbf{K} = [\kappa_1 \quad \kappa_2 \quad \kappa_3]^T$, or any other polynomial containing higher-order terms.

Theorem 2. *The dynamic feedback controller in Fig. 2, with $\mathbf{G}_w(z; \mathbf{d})$ and $\mathbf{f}_n(\cdot)$ satisfying Assumptions DC1 and DC2, modifies the characteristics of the N–S bifurcation exhibited by S preserving the location and stability of the fixed points. The stability of the emerging orbits is given by $\sigma_c = \sigma + \sigma_n$, where σ is the stability index of S and σ_n depends on $\mathbf{f}_n(\cdot)$, $\mathbf{K}$ and $\mathbf{d}$.*

Proof. Considering a unique vector $\mathbf{y}_k^c = [\mathbf{y}_k^T \quad (\mathbf{y}_k^w)^T]^T \in \mathbf{R}^{2m}$, the controlled system in Fig. 2 can be recast as that shown in Fig. 1, where now

$$\mathbf{G}_c(z; \boldsymbol{\mu}; \mathbf{d}) = \begin{bmatrix} \mathbf{I}_m \\ \mathbf{G}_w(z; \mathbf{d}) \end{bmatrix} \mathbf{G}(z; \boldsymbol{\mu}), \tag{1}$$

$$\mathbf{f}_c(\mathbf{y}_k^c; \boldsymbol{\mu}; \mathbf{K}) = \mathbf{f}(\mathbf{y}_k; \boldsymbol{\mu}) + \mathbf{f}_n(\mathbf{y}_k^w; \mathbf{K}), \tag{2}$$

with $\mathbf{I}_m$ being the $m \times m$ identity matrix. Hence, the discrete-time system (1)–(2) can be analyzed by using the FD approach of Section 2.

Since $\mathbf{y}_k^w = \mathbf{0}$ under steady state conditions ($z = 1$) and $\mathbf{f}_n(\mathbf{0}; \mathbf{K}) = \mathbf{0}$, the fixed points of S do not change so that $\widehat{\mathbf{y}}_c = [\widehat{\mathbf{y}} \quad \mathbf{0}]^T$. Due to the composition of $\mathbf{f}(\cdot)$ and $\mathbf{f}_n(\cdot)$, the Jacobian of $\mathbf{f}_c(\cdot)$ in a neighborhood of $\widehat{\mathbf{y}}_c$ can be written as $\mathbf{J}_c(\boldsymbol{\mu}; \mathbf{K}) = [\mathbf{J}(\boldsymbol{\mu}) \quad \mathbf{J}_n(\mathbf{K})]$. By Assumption DC2, $\mathbf{J}_n(\mathbf{K}) = D_y\mathbf{f}_n(\mathbf{0}; \mathbf{K}) = \mathbf{0}$ and then $\mathbf{J}_c(\boldsymbol{\mu}) = [\mathbf{J}(\boldsymbol{\mu}) \quad \mathbf{0}]$. Therefore,

$$\mathbf{G}_c(z; \boldsymbol{\mu}; \mathbf{d})\mathbf{J}_c(\boldsymbol{\mu}) = \begin{bmatrix} \mathbf{G}(z; \boldsymbol{\mu})\mathbf{J}(\boldsymbol{\mu}) & \mathbf{0} \\ \mathbf{G}_w(z; \mathbf{d})\mathbf{G}(z; \boldsymbol{\mu})\mathbf{J}(\boldsymbol{\mu}) & \mathbf{0} \end{bmatrix}, \tag{3}$$

and its characteristic polynomial is given by

$$\begin{aligned} P_o^c(\lambda; z; \boldsymbol{\mu}; \mathbf{d}) &= \det[\lambda\mathbf{I}_{2m} - \mathbf{G}_c(z; \boldsymbol{\mu}; \mathbf{d})\mathbf{J}_c(\boldsymbol{\mu})] \\ &= \lambda^m \det[\lambda\mathbf{I}_m - \mathbf{G}(z; \boldsymbol{\mu})\mathbf{J}(\boldsymbol{\mu})] = 0. \end{aligned}$$

Thus, m eigenvalues are zero and the rest are the roots of the original characteristic polynomial $P_o(\lambda; z; \boldsymbol{\mu}) = \det[\lambda\mathbf{I}_m - \mathbf{G}(z; \boldsymbol{\mu})\mathbf{J}(\boldsymbol{\mu})] = 0$, preserving the stability of $\widehat{\mathbf{y}}$. However, if $\widehat{\lambda}(e^{i\omega}; \boldsymbol{\mu})$ is a simple root of $P_o(\lambda; z; \boldsymbol{\mu})$ satisfying $\widehat{\lambda}(e^{i\omega}; \boldsymbol{\mu}) = -1 + i0$ for $\boldsymbol{\mu} = \boldsymbol{\mu}_o$ and $\omega = \omega_o$ ($e^{in\omega_o} \neq 1$ $n = 1, 2, 3, 4$) then $\widehat{\lambda}(e^{i\omega}; \boldsymbol{\mu})$ will also be a root of $P_o^c(\lambda; z; \boldsymbol{\mu})$. This N–S bifurcation point can not be eliminated or moved to a different position in the $\boldsymbol{\mu} - \omega$ space.

The characteristics of the orbits emerging from the bifurcation can be analyzed by applying Theorem 1, via the calculations in Table 1. Based on (3), the right and left eigenvectors (Step 1) associated with $\widehat{\lambda}(\cdot)$ are

$$\mathbf{v}^c = \begin{bmatrix} \mathbf{v} \\ \mathbf{v}^n \end{bmatrix} = \begin{bmatrix} \mathbf{I}_m \\ \mathbf{G}_w(z; \mathbf{d}) \end{bmatrix} \mathbf{v}, \qquad \mathbf{u}_c^T = [\mathbf{u}^T \quad \mathbf{0}]. \tag{4}$$

From Step 2, $\mathbf{H}_c(z; \boldsymbol{\mu}; \mathbf{d})$ is given by

$$\mathbf{H}_c(z; \boldsymbol{\mu}; \mathbf{d}) = \begin{bmatrix} \mathbf{I}_m \\ \mathbf{G}_w(z; \mathbf{d}) \end{bmatrix} \mathbf{H}(z; \boldsymbol{\mu}), \tag{5}$$

where $\mathbf{H}(z; \boldsymbol{\mu}) = [\mathbf{I}_m + \mathbf{G}(z; \boldsymbol{\mu})\mathbf{J}(\boldsymbol{\mu})]^{-1}\mathbf{G}(z; \boldsymbol{\mu})$. For matrix $\mathbf{Q}_c = \{q_{ij}^c\}$ in Step 3, it is possible to distinguish a part of q_{ij}^c depending on the second derivatives of $\mathbf{f}(\cdot)$ and another one depending on the second derivatives of $\mathbf{f}_n(\cdot)$, i.e.

$$q_{ij}^c = \begin{cases} \displaystyle\sum_{p=1}^m D_{y^p y^j}^2 f^i(\widehat{\mathbf{y}}; \boldsymbol{\mu}) v_p^c, & \text{for } 1 \le j \le m, \\ \displaystyle\sum_{p=m+1}^{2m} D_{y^p y^j}^2 f_n^i(\mathbf{0}; \mathbf{K}) v_p^c, & \text{for } m+1 \le j \le 2m. \end{cases}$$

Hence, $\mathbf{Q}_c$ can be represented as the block matrix

$$\mathbf{Q}_c = [\mathbf{Q} \quad \mathbf{Q}_n] = [D_{\mathbf{y}}^2\mathbf{f}(\widehat{\mathbf{y}}; \boldsymbol{\mu})\mathbf{v} \quad D_{\mathbf{y}}^2\mathbf{f}_n(\mathbf{0}; \mathbf{K})\mathbf{v}^n]. \tag{6}$$

Matrix $\mathbf{L}_c = D_{\mathbf{y}}^3\mathbf{f}_c(\widehat{\mathbf{y}}_c; \boldsymbol{\mu}; \mathbf{K})\mathbf{v}^c \otimes \mathbf{v}^c$ shows the same structure. Since

$$l_{ij}^c = \begin{cases} \displaystyle\sum_{p=1}^m \sum_{q=1}^m D_{y^p y^q y^j}^3 f^i(\widehat{\mathbf{y}}; \boldsymbol{\mu}) v_p^c v_q^c & \text{for } 1 \le j \le m, \\ \displaystyle\sum_{p=m+1}^{2m} \sum_{q=m+1}^{2m} D_{y^p y^q y^j}^3 f_n^i(\mathbf{0}; \mathbf{K}) v_p^c v_q^c & \text{for } m+1 \le j \le 2m, \end{cases}$$

then,

$$\mathbf{L}_c = [\mathbf{L} \quad \mathbf{L}_n] = [D_{\mathbf{y}}^3\mathbf{f}(\widehat{\mathbf{y}}; \boldsymbol{\mu})\mathbf{v} \otimes \mathbf{v} \quad D_{\mathbf{y}}^3\mathbf{f}_n(\mathbf{0}; \mathbf{K})\mathbf{v}^n \otimes \mathbf{v}^n]. \tag{7}$$

According to (4)–(6), vectors $\mathbf{v}_0^c$ and $\mathbf{v}_2^c$ in Step 4 are

$$\mathbf{v}_0^c = \begin{bmatrix} \mathbf{v}_0 + \mathbf{v}_0^n \\ \mathbf{0} \end{bmatrix}, \qquad \mathbf{v}_2^c = \begin{bmatrix} \mathbf{I}_m \\ \mathbf{G}_w(e^{i2\omega}; \mathbf{d}) \end{bmatrix} (\mathbf{v}_2 + \mathbf{v}_2^n), \tag{8}$$

where $\mathbf{v}_0^n = -\mathbf{H}(1; \boldsymbol{\mu})\mathbf{Q}_n\overline{\mathbf{v}}^n/4$, $\mathbf{v}_2^n = -\mathbf{H}(e^{i2\omega}; \boldsymbol{\mu})\mathbf{Q}_n\mathbf{v}^n/4$ and $\mathbf{v}_0, \mathbf{v}_2$ are the vectors corresponding to system S. Based on these expressions and (7), vector $\mathbf{p}^c(\omega; \boldsymbol{\mu}; \mathbf{d}; \mathbf{K})$ is

$$\mathbf{p}^c(\omega; \boldsymbol{\mu}; \mathbf{d}; \mathbf{K}) = \mathbf{p}(\omega; \boldsymbol{\mu}) + \mathbf{p}^n(\omega; \boldsymbol{\mu}; \mathbf{d}; \mathbf{K}), \tag{9}$$

where again $\mathbf{p}(\omega; \boldsymbol{\mu})$ is associated with S and

$$\begin{aligned} \mathbf{p}^n(\omega; \boldsymbol{\mu}; \mathbf{d}; \mathbf{K}) &= \mathbf{Q}\mathbf{v}_0^n + \frac{1}{2}\overline{\mathbf{Q}}\mathbf{v}_2^n + \frac{1}{8}\mathbf{L}^n\overline{\mathbf{v}}^n \\ &\quad + \frac{1}{2}\overline{\mathbf{Q}_n}\mathbf{G}_w(e^{i2\omega}; \mathbf{d})(\mathbf{v}_2 + \mathbf{v}_2^n). \end{aligned} \tag{10}$$

Coefficient $\xi^c(\cdot)$ in Step 5 can also be expressed as the sum of two terms. Since $\mathbf{u}_c^T\mathbf{G}_c(e^{i\omega}; \boldsymbol{\mu}; \mathbf{d}) = \mathbf{u}^T\mathbf{G}(e^{i\omega}; \boldsymbol{\mu})$ and $\mathbf{u}_c^T\mathbf{v}^c = \mathbf{u}^T\mathbf{v}$, $\xi^c(\omega; \boldsymbol{\mu}; \mathbf{d}; \mathbf{K}) = \xi(\omega; \boldsymbol{\mu}) + \xi^n(\omega; \boldsymbol{\mu}; \mathbf{d}; \mathbf{K})$ with $\xi^n(\omega; \boldsymbol{\mu}; \mathbf{d}; \mathbf{K}) = -\mathbf{u}^T\mathbf{G}(e^{i\omega}; \boldsymbol{\mu})\mathbf{p}^n(\omega; \boldsymbol{\mu}; \mathbf{d}; \mathbf{K})/(\mathbf{u}^T\mathbf{v})$. Now, if the Nyquist diagram of $\widehat{\lambda}(e^{i\omega}; \boldsymbol{\mu})$ intersects the new curve $-1 + \xi^c(\omega; \boldsymbol{\mu}; \mathbf{d}; \mathbf{K})\theta^2$, the controlled system also presents an invariant orbit around $\widehat{\mathbf{y}}_c$ (Step 6). Amplitude θ and frequency ω of this oscillation depend not only on $\boldsymbol{\mu}$ but also on the washout-filter poles $\mathbf{d}$ and the gain vector $\mathbf{K}$.

Up to this point, the obtained results do not permit a direct control over the stability of the orbits. Taking into account that $\mathbf{u}_c^T D_z\mathbf{G}_c(e^{i\omega}; \boldsymbol{\mu}; \mathbf{d}) = \mathbf{u}^T D_z\mathbf{G}(e^{i\omega}; \boldsymbol{\mu})$ and $\mathbf{J}_c(\boldsymbol{\mu})\mathbf{v}^c = \mathbf{J}(\boldsymbol{\mu})\mathbf{v}$, it results that $\boldsymbol{\gamma}_c = \boldsymbol{\gamma}$, and the stability index given in Step 8 is given by $\sigma_c = \text{Re}\{\boldsymbol{\gamma}\mathbf{p}^c(\omega; \boldsymbol{\mu}; \mathbf{d}; \mathbf{K})\}$ for $\boldsymbol{\mu} = \boldsymbol{\mu}_o$ and $\omega = \omega_o$. Finally, substituting (9) into this equation gives $\sigma_c = \sigma + \sigma_n$ with

$$\sigma_n = \text{Re}\{\boldsymbol{\gamma}_o\mathbf{p}^n(\omega_o; \boldsymbol{\mu}_o; \mathbf{d}; \mathbf{K})\}, \qquad \boldsymbol{\gamma}_o = \boldsymbol{\gamma}|_{\boldsymbol{\mu}=\boldsymbol{\mu}_o, \omega=\omega_o}. \tag{11}$$

Index σ_c reveals that the proposed controller adds a correction term σ_n to the stability index σ of S. Thus, a properly chosen function $\mathbf{f}_n(\cdot)$ together with vectors $\mathbf{K}$ and $\mathbf{d}$ makes it possible to control the sign of σ_c and, consequently, the type of N–S bifurcation presented by the system. $\square$

A degenerate N–S bifurcation ($\sigma = 0$) can be transformed into a supercritical (subcritical) one by defining $\mathbf{f}_n(\cdot)$, $\mathbf{K}$ and $\mathbf{d}$ such that $\sigma_n > 0$ ($\sigma_n < 0$). When σ and σ_n share the same sign, $|\sigma_c| > |\sigma|$ and the controlled system will be farther from a degeneracy. As will be illustrated below, the manipulation of σ_c also provides a means of modifying the amplitude of the orbits. In fact, as $|\sigma_c|$ increases the branches of the bifurcation grow more gradually, improving its stability characteristics. On the contrary, when the signs of σ and σ_n are opposite, $|\sigma_c| < |\sigma|$, and the amplitude of the orbit increases more abruptly, deteriorating the stability of the bifurcation.

3.2. Static controller

If explicit and exact expressions of all fixed points of the system are available, the control loop proposed in Section 3.1 can be simplified to that shown in Fig. 3. In this case, the controller is only composed of a nonlinear static function which depends only on $\mathbf{y}_k$.
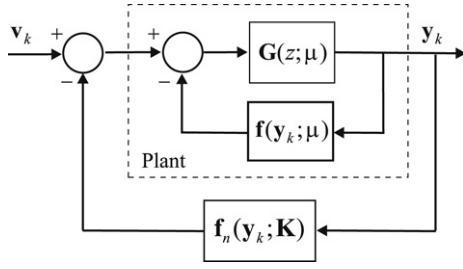
Fig. 3. Block diagram of the static feedback controller.

Assumption SC1. The static function $\mathbf{f}_n(\mathbf{y}_k; \mathbf{K}) : \mathbf{R}^m \times \mathbf{R}^v \rightarrow \mathbf{R}^\ell$ of Fig. 3 satisfies: (i) it is at least C^3 in its first argument; (ii) $\mathbf{f}_n(\widehat{\mathbf{y}}_j; \mathbf{K}) = \mathbf{0} \, \forall \widehat{\mathbf{y}}_j$, (iii) $D_{\mathbf{y}} \mathbf{f}_n(\widehat{\mathbf{y}}_j; \mathbf{K}) = \mathbf{0} \, \forall \widehat{\mathbf{y}}_j$, where $\widehat{\mathbf{y}}_j$ stands for any of the fixed point of S.

As an example, if $\mathbf{y}_k = [\, y_k^1 \quad y_k^2 \,]^T$ and $\widehat{\mathbf{y}} = [\widehat{y}^1 \quad \widehat{y}^2]^T$ is the unique fixed point of the system, a possible selection of $\mathbf{f}_n(\cdot)$ could be the homogeneous polynomial $\mathbf{f}_n(\mathbf{y}_k; \mathbf{K}) = \kappa_1(y_k^1 - \widehat{y}^1)^2 + \kappa_2(y_k^2 - \widehat{y}^2)^2 + \kappa_3(y_k^1 - \widehat{y}^1)(y_k^2 - \widehat{y}^2)$ where $\mathbf{K}$ is the gain vector $\mathbf{K} = [\kappa_1 \quad \kappa_2 \quad \kappa_3]^T$.

According to Assumption SC1, function $\mathbf{f}_n(\cdot)$ (and its derivative with respect to $\mathbf{y}_k$) vanishes at every operating point of S; the dynamic controller of Section 3.1, however, requires that the nonlinear function (and its derivative with respect to $\mathbf{y}_k^w$) vanishes only at the origin (Assumption DC2).

Theorem 3. *The static controller of Fig. 3 with function $\mathbf{f}_n(\cdot)$ satisfying Assumption SC1 changes the characteristics of the N–S bifurcation exhibited by S while preserving the location and stability of its fixed points. The stability of the emerging orbits is determined by $\sigma_c = \sigma + \sigma_n$, where σ is the stability index of S and σ_n depends on function $\mathbf{f}_n(\cdot)$ and the gain vector $\mathbf{K}$.*

Proof. The system depicted in Fig. 3 can be transformed into that of Fig. 1 considering $\mathbf{G}_c(z; \boldsymbol{\mu}) = \mathbf{G}(z; \boldsymbol{\mu})$ and $\mathbf{f}_c(\mathbf{y}_k; \boldsymbol{\mu}; \mathbf{K}) = \mathbf{f}(\mathbf{y}_k; \boldsymbol{\mu}) + \mathbf{f}_n(\mathbf{y}_k; \mathbf{K})$. Therefore, it is possible to apply the methodology of Section 2 to study its N–S bifurcation.

By Assumption SC1, $\mathbf{f}_n(\widehat{\mathbf{y}}; \mathbf{K}) = \mathbf{0}$ so that $\widehat{\mathbf{y}}_c = \widehat{\mathbf{y}}$ (the fixed points remains unchanged). The linearization of $\mathbf{f}_c(\cdot)$ in a neighborhood of $\widehat{\mathbf{y}}$ is given by $\mathbf{J}_c(\boldsymbol{\mu}; \mathbf{K}) = \mathbf{J}(\boldsymbol{\mu}) + \mathbf{J}_n(\mathbf{K})$. Since $\mathbf{J}_n(\mathbf{K}) = D_{\mathbf{y}} \mathbf{f}_n(\widehat{\mathbf{y}}; \mathbf{K}) = \mathbf{0}$, the Jacobian is $\mathbf{J}_c(\boldsymbol{\mu}; \mathbf{K}) = \mathbf{J}(\boldsymbol{\mu})$ and thus, $\mathbf{G}_c(z; \boldsymbol{\mu}) \mathbf{J}_c(\boldsymbol{\mu}) = \mathbf{G}(z; \boldsymbol{\mu}) \mathbf{J}(\boldsymbol{\mu})$, with its characteristic polynomial $P_o^c(\lambda; z; \boldsymbol{\mu}) = \det[\lambda \mathbf{I}_m - \mathbf{G}(z; \boldsymbol{\mu}) \mathbf{J}(\boldsymbol{\mu})] = 0$. As before, the controller maintains not only the stability of $\widehat{\mathbf{y}}$ but also its critical points. In fact, since $\widehat{\lambda}(e^{i\omega}; \boldsymbol{\mu})$ is a root of $P_o^c(\lambda; z; \boldsymbol{\mu})$ such that $\widehat{\lambda}(e^{i\omega}; \boldsymbol{\mu}) = -1 + i0$ for $\boldsymbol{\mu} = \boldsymbol{\mu}_o$ and $\omega = \omega_o$ ($e^{in\omega_o} \neq 1$ $n = 1, 2, 3, 4$), the controlled system also undergoes a N–S bifurcation.

Again, the orbits emerging from the bifurcation can be studied by applying Theorem 1. In this case, it is easy to see that $\mathbf{v}^c = \mathbf{v}$, $\mathbf{u}_c^T = \mathbf{u}^T$ and $\mathbf{H}_c(z; \boldsymbol{\mu}) = \mathbf{H}(z; \boldsymbol{\mu})$. Due to the composition of $\mathbf{f}_c(\cdot)$, matrix $\mathbf{Q}_c$ (in Step 3 of Table 1) can be directly computed as $\mathbf{Q}_c = \mathbf{Q} + \mathbf{Q}_n$ with $\mathbf{Q}_n = D_{\mathbf{y}}^2 \mathbf{f}_n(\widehat{\mathbf{y}}; \mathbf{K}) \mathbf{v}$. In the same way, $\mathbf{L}_c = \mathbf{L} + \mathbf{L}_n$, where $\mathbf{L}_n = D_{\mathbf{y}}^3 \mathbf{f}_n(\widehat{\mathbf{y}}; \mathbf{K}) \mathbf{v} \otimes \mathbf{v}$. Following Step 4, vectors $\mathbf{v}_0^c$ and $\mathbf{v}_2^c$ are given by $\mathbf{v}_0^c = \mathbf{v}_0 + \mathbf{v}_0^n$ and $\mathbf{v}_2^c = \mathbf{v}_2 + \mathbf{v}_2^n$ with $\mathbf{v}_0^n = -\mathbf{H}(1; \boldsymbol{\mu}) \mathbf{Q}_n \overline{\mathbf{v}}/4$ and $\mathbf{v}_2^n = -\mathbf{H}(e^{i2\omega}; \boldsymbol{\mu}) \mathbf{Q}_n \mathbf{v}/4$. Similarly,

$$\mathbf{p}^c(\omega; \boldsymbol{\mu}; \mathbf{K}) = \mathbf{p}(\omega; \boldsymbol{\mu}) + \mathbf{p}^n(\omega; \boldsymbol{\mu}; \mathbf{K}), \tag{12}$$

where

$$\mathbf{p}^n(\omega; \boldsymbol{\mu}; \mathbf{K}) = \mathbf{Q}\mathbf{v}_0^n + \frac{1}{2}\overline{\mathbf{Q}}\mathbf{v}_2^n + \mathbf{Q}_n(\mathbf{v}_0 + \mathbf{v}_0^n)$$
$$+ \frac{1}{2}\overline{\mathbf{Q}}_n(\mathbf{v}_2 + \mathbf{v}_2^n) + \frac{1}{8}\mathbf{L}^n \overline{\mathbf{v}}. \tag{13}$$

As in the proof of Theorem 2, the structure of $\mathbf{p}^c(\cdot)$ reveals that coefficient $\xi^c(\cdot)$ in Step 5 can be written as the sum of two terms, $\xi^c(\omega; \boldsymbol{\mu}; \mathbf{K}) = \xi(\omega; \boldsymbol{\mu}) + \xi^n(\omega; \boldsymbol{\mu}; \mathbf{K})$ with $\xi^n(\omega; \boldsymbol{\mu}; \mathbf{K}) = -\mathbf{u}^T \mathbf{G}(e^{i\omega}; \boldsymbol{\mu}) \mathbf{p}^n(\omega; \boldsymbol{\mu}; \mathbf{K})/(\mathbf{u}^T \mathbf{v})$. Then, if condition $\widehat{\lambda}(e^{i\omega}; \boldsymbol{\mu}) = -1 + \xi^c(\omega; \boldsymbol{\mu}; \mathbf{K})\theta^2$ is satisfied, the controlled system exhibits an invariant orbit around $\widehat{\mathbf{y}}_c$ in which the amplitude θ and the frequency ω can be altered by varying $\xi^n(\cdot)$.

Based on (12) and noticing that $\boldsymbol{\gamma}_c = \boldsymbol{\gamma}$, the stability index of Step 8 results in $\sigma_c = \sigma + \sigma_n$ with

$$\sigma_n = \text{Re}\{\boldsymbol{\gamma}_o \mathbf{p}^n(\omega_o; \boldsymbol{\mu}_o; \mathbf{K})\}, \qquad \boldsymbol{\gamma}_o = \boldsymbol{\gamma}|_{\boldsymbol{\mu}=\boldsymbol{\mu}_o, \omega=\omega_o}. \tag{14}$$

As before, a proper selection of function $\mathbf{f}_n(\cdot)$ and gain vector $\mathbf{K}$ makes it possible to control the N–S bifurcation presented by the system. $\quad\square$

4. A simple example

The control of the emerging orbits of a N–S bifurcation is illustrated with the classical delayed logistic map. This system has been extensively analyzed and controlled in the literature. For instance, a quadratic law is used in [5] to manipulate the location of the bifurcation. A cubic law is derived in [12] to control a modified version of the delayed logistic map. In this case, the complexity of the FD design is comparable with that of the time-domain methods presented in the mentioned works.

The delayed logistic map is given by

$$\begin{cases} x_{k+1}^1 = x_k^2, \\ x_{k+1}^2 = \mu x_k^2(1 - x_k^1). \end{cases}$$

This map has two fixed points: $\widehat{\mathbf{y}}_0 = \mathbf{0}$ and $\widehat{\mathbf{y}}_1 = (1 - 1/\mu)[1 \quad 1]^T$. Point $\widehat{\mathbf{y}}_1$ is unstable for $0 < \mu < 1$ and stable for $1 < \mu < 2$, undergoing a N–S bifurcation at $\mu_o = 2$ ($\omega_o = \pi/3$). As shown in [19], this system can be recast in the form of Fig. 1 with $\mathbf{G}(z; \mu) = (z - \mu)^{-1}[z^{-1} \quad 1]^T$ and $f(\mathbf{y}_k; \mu) = \mu y_k^1 y_k^2$. The nonzero eigenvalue associated with $\widehat{\mathbf{y}}_1$ is $\widehat{\lambda}(z; \mu) = (\mu - 1)(1 + z^{-1})(z - \mu)^{-1}$. Applying Theorem 1, it is found that $\sigma = 0.5$, indicating that the bifurcation is supercritical. Table 2 reports the vectors related to the system.

Now, the proposed control strategies are used to change the characteristics of the orbits. Although $\mathbf{y}_k$ is a two-dimensional vector, only the state y_k^2 is considered for bifurcation control, *i.e.* $\mathbf{f}_n(\cdot)$ is chosen as a scalar function.

Dynamic controller. Based on Assumptions DC1 and DC2, blocks are chosen as $\mathbf{f}_n(\cdot) = \kappa(y_k^{w,2})^2$ and

$$\mathbf{G}_w(z; d) = \begin{bmatrix} 0 & 0 \\ 0 & g_{22} \end{bmatrix}, \qquad g_{22} = \frac{z - 1}{z - 1 + d}.$$

Vectors necessary to calculate (10) can be found in Table 2. Evaluating $\mathbf{p}^n(\cdot)$ at $\mu_o = 2$ and $\omega_o = \pi/3$, the correction term (11) of Theorem 2 is given by

$$\sigma_n = \frac{(3 - 7d + 8d^2 - 5d^3 + d^4)\kappa + d(2 - d)\kappa^2}{4(3 - 9d + 16d^2 - 17d^3 + 12d^4 - 5d^5 + d^6)},$$

meaning that the stability of the N–S bifurcation can be altered by varying feedback gain κ and filter parameter d. As is illustrated by the solid curves in Fig. 4, the same σ_n value can be obtained with several pairs of (κ, d). So, an additional criterion for fixing these parameters can be, for instance, to minimize the feedback gain of the controller for a given σ_n. Since the maximum gain of the washout filter occurs at $z = -1$, its upper limit is $g_c = \kappa g_{22}|_{z=-1} = 2\kappa/(2 - d)$. Level curves of g_c in terms of κ and d are shown by dashed lines in Fig. 4. The minimum value is attained when the line of g_c is tangent to the curve σ_n. Hence, for example, the optimal combination of κ and d for obtaining $\sigma_{nd} = 0.5$ with the minimum feedback gain is $\kappa = 1.15748$ and

Table 2
Vectors related to the control of the delayed logistic map.

Original system	$\mathbf{v} = \begin{bmatrix} \frac{1}{z} & 1 \end{bmatrix}^T \quad \mathbf{u}^T = \begin{bmatrix} 1 & 1 \end{bmatrix}$
	$\mathbf{H}(z;\mu) = \frac{1}{z^2 - z + \mu - 1} \begin{bmatrix} 1 & z \end{bmatrix}^T$
	$\mathbf{Q} = \mu \begin{bmatrix} 1 & \frac{1}{z} \end{bmatrix} \quad \mathbf{L} = \begin{bmatrix} 0 & 0 \end{bmatrix}$
	$\mathbf{v}_0 = \frac{\mu \mathrm{Re}\{z\}}{2(1-\mu)|z|^2} \begin{bmatrix} 1 & 1 \end{bmatrix}^T, \qquad \mathbf{v}_2 = \frac{\mu}{2z} \mathbf{H}(z^2;\mu)$
	$\mathbf{p}(\omega_o;\mu_o) = \mathrm{i}\frac{-3+\sqrt{3}}{2}, \qquad \boldsymbol{\gamma}_o = -\mathrm{i}\frac{\sqrt{3}}{3}$
Dynamic controller	$\mathbf{v}^n = \begin{bmatrix} 0 & g_{22} \end{bmatrix}^T$
	$\mathbf{Q}_n = \begin{bmatrix} 0 & 2\kappa g_{22} \end{bmatrix} \quad \mathbf{L}_n = \begin{bmatrix} 0 & 0 \end{bmatrix}$
	$\mathbf{v}_0^n = \frac{\kappa(1 - \mathrm{Re}\{z\})}{(1-\mu)[(1-d)^2 + 2(d-1)\mathrm{Re}\{z\} + 1]} \begin{bmatrix} 1 & 1 \end{bmatrix}^T$
	$\mathbf{v}_2^n = -\frac{\kappa g_{22}^2}{2} \mathbf{H}(z^2;\mu)$
Static controller	$\mathbf{Q}_n = \begin{bmatrix} 0 & 2\kappa(1 - \frac{1}{\mu})^2 \end{bmatrix} \quad \mathbf{L}_n = \begin{bmatrix} 0 & 12\kappa(1 - \frac{1}{\mu}) \end{bmatrix}$
	$\mathbf{v}_0^n = \frac{(1-\mu)\kappa}{2\mu^2} \begin{bmatrix} 1 & 1 \end{bmatrix}^T$
	$\mathbf{v}_2^n = -\frac{(1-\mu)^2 \kappa}{2\mu^2 (z^4 - z^2 - 1 + \mu)} \begin{bmatrix} 1 & z^2 \end{bmatrix}^T$
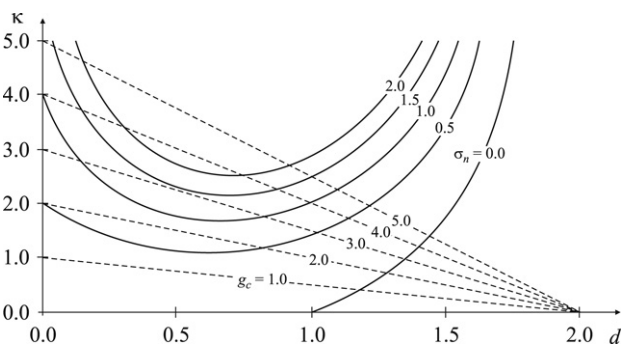
Fig. 4. Level curves of constant σ_n values (solid lines) and constant feedback gain g_c (dashed lines) as functions of κ and d.
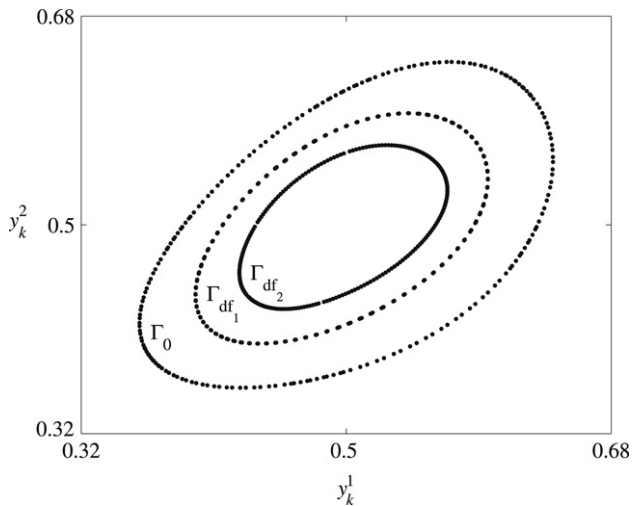

Fig. 5. Invariant orbits for $\mu = 2.02$ and different κ and d values of the dynamic controller: $(\Gamma_0)\,\kappa = 0$; $(\Gamma_{df_1})\,\kappa = 1.15748$, $d = 0.41675$; $(\Gamma_{df_2})\,\kappa = 2.23981$, $d = 0.50665$.

$d = 0.41675$ ($g_{c\,\min} = 1.46215$). In the same way, the optimal pair corresponding to $\sigma_{nd} = 1.5$ is $\kappa = 2.23981$ and $d = 0.50665$ ($g_{c\,\min} = 2.99971$).

Fig. 5 shows the changes in the oscillations of the controlled map for $\mu = 2.02$ and the κ and d values obtained above: (Γ_0) $\sigma_c = \sigma = 0.5$ (open-loop system with $\kappa = 0$); $(\Gamma_{df_1})\,\sigma_c = 1 > 0.5$ ($\kappa = 1.15748$, $d = 0.41675$); and $(\Gamma_{df_2})\,\sigma_c = 2 > 1$ ($\kappa = 2.23981$, $d = 0.50665$). The proposed controller allows a precise manipulation of the system dynamics: larger σ_c values lead to smaller orbits around $\widehat{\mathbf{y}}_1$, as predicted by theoretical analysis.
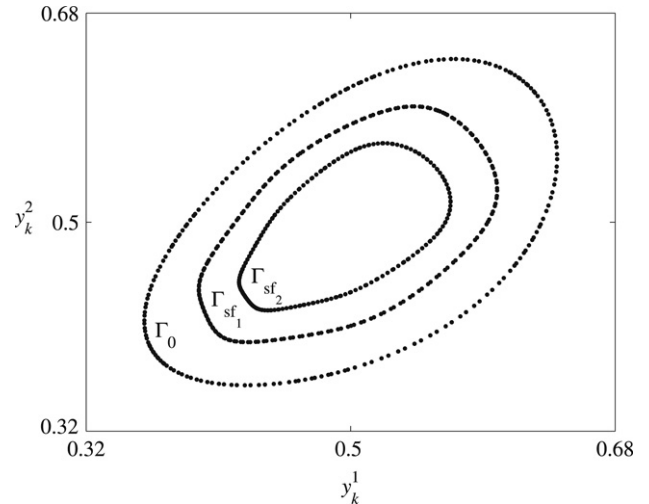

Fig. 6. Invariant orbits for $\mu = 2.02$ and different κ values of the static controller: $(\Gamma_0)\,\kappa = 0$; $(\Gamma_{sf_1})\,\kappa = 8$; $(\Gamma_{sf_2})\,\kappa = 24$.

Static controller. Taking into account Assumption SC1, the nonlinear function is chosen as $\mathbf{f}_n(\cdot) = \kappa(y_k^2)^2(y_k^2 - 1 + \mu^{-1})^2$. According to the vectors in Table 2, the evaluation of (13) at the critical point ($\mu_o = 2$, $\omega_o = \pi/3$) results in $\mathbf{p}^n(\omega_o;\mu_o;\kappa) = \kappa/64(12 - 3\kappa + 4\sqrt{3}\mathrm{i})$. Since $\boldsymbol{\gamma}_o = -\mathrm{i}\sqrt{3}/3$, the correction term (14) is given by $\sigma_n = \kappa/16$. Therefore, from Theorem 3, the index of the controlled system is $\sigma_c = 1/2 + \kappa/16$. The orbits presented by the controlled delayed logistic map for $\mu = 2.02$ are depicted in Fig. 6. In this case, the κ values are: $(\Gamma_0)\,\kappa = 0$ (open-loop system with $\sigma = 0.5$); $(\Gamma_{sf_1})\,\kappa = 8$ ($\sigma_c = 1 > 0.5$); and $(\Gamma_{sf_2})\,\kappa = 24$ ($\sigma_c = 2 > 1$). Again, larger σ_c values lead to smaller orbits around $\widehat{\mathbf{y}}_1$.

5. Conclusions

Two FD methods for controlling the basic characteristics of the oscillations exhibited by a discrete-time system due to Neimark–Sacker bifurcation have been presented. The first one adds to the original system an outer feedback loop consisting of a washout filter and a nonlinear static function. The second one uses only a nonlinear static feedback, but requires the knowledge of all the equilibria of the system to preserve their locations and stability. In both cases, the parameters of the controllers are chosen according to the desired value of the stability index of the bifurcation. The procedure is illustrated with a simple numerical example. The proposed bifurcation control in the frequency-domain offers an alternative to the traditional methodologies in the time-domain.

References

[1] Y.A. Kuznetsov, Elements of Applied Bifurcation Theory, Springer-Verlag, New York, 1995.
[2] G. Chen, X. Dong, From Chaos to Order: Methodologies, Perspectives and Applications, vol. 24 Serie A, World Scientific Publishing Co., Singapore, 1998.
[3] G. Chen, J.L. Moiola, H.O. Wang, Bifurcation control: Theories, methods and applications, Internat. J. Bifur. Chaos 10 (3) (2000) 511–548.
[4] A.J. Krener, W. Kang, D.E. Chang, Control bifurcations, IEEE Trans. Automat. Control 49 (8) (2004) 1231–1246.
[5] Z. Chen, P. Yu, Controlling and anti-controlling Hopf bifurcations in discrete maps using polynomial functions, Chaos Solitons Fractals 26 (2005) 1231–1248.
[6] P. Yu., G. Chen, Hopf bifurcation control using nonlinear feedback with polynomial functions, Internat. J. Bifur. Chaos 14 (5) (2004) 1683–1704.
[7] H.C. Lee, Robust control of bifurcating nonlinear systems with applications, Ph.D. Thesis, University of Maryland, USA, 1991.
[8] H.O. Wang, E.H. Abed, Bifurcation control of chaotic system, Automatica 31 (9) (1995) 1213–1226.

[9] E.H. Abed, J.H. Fu, Local feedback stabilization and bifurcation control, I. Hopf bifurcation, Systems Control Lett. 7 (1986) 11–17.

[10] E.H. Abed, J.H. Fu, Local feedback stabilization and bifurcation control, II. Stationary bifurcation, Systems Control Lett. 8 (1987) 467–473.

[11] E.H. Abed, H.O. Wang, R.C. Chen, Stabilization of period doubling bifurcations and implications for control of chaos, Physica D 70 (1–2) (1994) 154–164.

[12] H. Yaghoobi, E.H. Abed, Local feedback control of the Neimark–Sacker bifurcation, Internat. J. Bifur. Chaos 13 (4) (2003) 879–893.

[13] B. Hamzi, J. Barbot, S. Monaco, D. Normand-Cirot, Nonlinear discrete-time control of systems with a Neimark–Sacker bifurcation, Systems Control Lett. 44 (2001) 245–258.

[14] B. Hamzi, A.J. Krener, W. Kang, The controlled center dynamics of discrete time control bifurcations, Systems Control Lett. 55 (2006) 585–596.

[15] A.J. Krener, L. Li, Normal forms and bifurcations of discrete time nonlinear control systems, SIAM J. Control Optim. 40 (6) (2002) 1697–1723.

[16] G. Wen, D. Xu, Control of degenerate Hopf bifurcations in three-dimensional maps, Chaos 13 (2) (2003) 486–494.

[17] G. Wen, D. Xu, X. Han, On the creation of Hopf bifurcations in discrete-time nonlinear systems, Chaos 12 (2) (2002) 350–355.

[18] G. Wen, D. Xu, X. Han, Controlling Hopf bifurcations of discrete-time systems in resonance, Chaos Solitons Fractals 23 (2005) 1865–1877.

[19] M.B. D'Amico, J.L. Moiola, E.E. Paolini, Hopf bifurcation for maps: A frequency domain approach, IEEE Trans. Circuits Syst. I 49 (3) (2002) 281–288.

[20] M.B. D'Amico, J.L. Moiola, E.E. Paolini, Study of degenerate bifurcations in maps: A feedback system approach, Internat. J. Bifur. Chaos 14 (5) (2004) 1625–1641.

[21] R.W. Brockett, The status of stability theory for deterministic systems, IEEE Trans. Automat. Control 11 (3) (1966) 596–606.

[22] B. Brogliato, R. Lozano, B. Maschke, O. Egeland, Dissipative Systems Analysis and Control: Theory and Applications, Springer Verlag, London, 2007.

[23] V. Kapila, W.M. Haddad, A multivariable extension of the Tsypkin criterion using a Lyapunov-function approach, IEEE Trans. Automat. Control 41 (1) (1996) 149–152.

[24] M.B. D'Amico, G. Chen, J.L. Moiola, E. Paolini, A frequency-analytic approach for controlling Neimark–Sacker bifurcations, in: 1st IFAC Conf. Analysis Control Chaotic Systems, Reims (France), 2006.

[25] D.J. Allwright, Harmonic balance and the Hopf bifurcation theorem, Math. Proc. Cambridge Philos. Soc. 82 (3) (1977) 453–467.

[26] A.I. Mees, Dynamics of Feedback Systems, John Wiley & Sons, New York, 1981.

[27] G. Agamennoni, G.L. Calandrini, J.L. Moiola, Some realizations in the study of oscillations with a frequency method, Dyn. Contin. Discrete Impuls. Syst. Ser. B Appl. Algorithms 11 (1) (2008) 99–110.